CPT-34
ORO-3992-141
August 1973

"A Diffractive Amplitude with Rising Total Cross Section"*

by

Charles B. Chiu

Center for Particle Theory

University of Texas

Austin, Texas 78712

R. J. Gleiser

I.M.A.F., Universidad Nacional de Cordoba

Cordoba, Argentina

and

Center for Particle Theory

University of Texas

Austin, Texas 78712

and

Kuo-Hsiang Wang

Center for Particle Theory

University of Texas

Austin, Texas 78712

*Work supported in part by the USAEC (40-1)3992.

Abstract

We propose a simple parameterization for high energy diffractive amplitude based on an absorbed multiperipheral model and the unitarity relation. This parameterization gives an eventual $\sim(\ln s)^2$ growth for the total cross section and a $\sim\ln s$ growth for the average multiplicity. This amplitude together with Regge pole contribution gives a good fit to the pp elastic scattering data for $p_{Lab} \gtrsim 10$ GeV/c and $|t| \lesssim 0.8$ GeV^2.

1. Introduction

Recent ISR data[1] indicate that pp total cross section increases as a function of c.m. collision energy ($\sqrt{s}$). Theoretically the rise of a total cross section with an asymptotic behavior $\sim(\ln s)^2$ is anticipated in the QED model of Cheng and Wu.[2] A similar rise is also expected from various eikonal models,[3,4] and absorbed multiperipheral models,[4,5,6] when a "strong coupling condition" is imposed. After the ISR data became available, the pp elastic data were analyzed by Cheng, Walker and Wu in terms of a simple parameterization based on an impact picture in accord with the earlier QED model.[7] To our knowledge, this is the only work advanced thus far, which gives a quantitative description to both the total cross section and the near forward scattering data. In this paper, we propose a different parameterization for the diffractive amplitude based on the idea of absorbed multiperipheral model and unitarity relation. This amplitude together with a Regge pole contribution gives a quantitative description to the pp data for $p_{Lab} \gtrsim 10$ GeV/c and $|t| \lesssim 0.8$ GeV^2. Our model predicts that ultimately the total cross section grows like $\sim(\ln s)^2$, while the average pion multiplicity grows like $\sim \ln s$.

2. The model.

For definiteness, we shall consider pp scattering only. However, most of our discussions below can be easily generalized to other cases. For large s the pp elastic amplitude, $T_{22} = T_{22}(s,b)$ at a given impact parameter b, satisfies following asymptotic unitarity relation

$$\begin{aligned} 2\ \mathrm{Im}T_{22} &= |\mathrm{Im}T_{22}|^2 + |\mathrm{Re}T_{22}|^2 + \sum_{N\geq 3} T_{2N}T_{2N}^{*} \\ &\equiv |\mathrm{Im}T_{22}|^2 + \sum_{N\geq 2} \tilde{T}_{2N}\tilde{T}_{2N}^{*} \quad . \end{aligned} \tag{1}$$

We shall ignore any spin effects. We assume that at high energies, the elastic scattering amplitude contains a diffractive term, which has a power behavior s^{0} up to some lns factor and is mainly imaginary, and a lower power term, with e.g. $\sim s^{-\frac{1}{2}}$. We approximate $\mathrm{Im}T_{22}$ by the leading diffractive contribution alone. On the right hand side of Eq. (1), the inelastic contribution is to be saturated by an "absorbed" multiperipheral series, with "proper" Regge trajectories (i.e. ω-f^{0}, ρ-A_2 with $\alpha = 0.5 + t$) exchanged along the multiperipheral chain. In the limit of exchange degeneracy, the exchange of α gives a real contribution to T_{22}.[8] So it is natural to include the $|\mathrm{Re}T_{22}|^2$ term in the sum, which was done in the last step of Eq. (1). Taking into account both the initial and final state absorptions between the two nucleon lines, Eq. (1) can be written as

$$2\ \mathrm{Im}T_{22} \geq |\mathrm{Im}T_{22}|^2 + |S_{22}|^2 H = |\mathrm{Im}T_{22}|^2 + |1 + iT_{22}|^2 H \quad , \quad (2)$$

where $H = H(s,b)$ is the unabsorbed overlap function. After a Fourier-Bessel transform, this overlap function at $t = 0$ is given by[9]

$$H(s,t=0) = \langle H(s,b)\rangle_o = FE^c \sum_{N=2}^{\infty} \sigma_N(g^2 \ln E)\ \langle G(N,b)\rangle_o = FE^c, \quad (3)$$

where the symbol $\langle\rangle$ designates a Fourier-Bessel transform, i.e.

$$H(s,t) \equiv \langle H(s,b)\rangle_t = \int_o^\infty b\,db\, H(s,b) J_o(xb), \text{ with } x = \sqrt{-t} \quad . \quad (4)$$

In Eq. (3) F is a parameter specifying the overall strength. E is the incident lab. energy in GeV, $E \approx s/2M$, with M being the nucleon mass. And $c = 2\alpha(0) - 2 + g^2 \approx g^2 - 1$. To give rise to an asymptotic behavior: s^o with positive power of $\ln s$ in the absorbed amplitude, it is necessary that c be positive, or equivalently the "strong coupling condition" to hold,[2-6] i.e.

$$g^2 > 2 - 2\alpha(0) \quad . \quad (5)$$

In general, resonances in addition to pions are expected to be emitted along the multiperipheral chain. So N in Eq. (3) specifies the total number of "particles" (pions, as well as resonances, and also the two nucleons) in the final state.

The number of particles emitted along the internal chain is N-2. In Eq. (3), σ_N is the normalized particle multiplicity distribution which depends on $g^2 \ell nE$. And G(N,b) is an unknown function, which specifies the production probability as a function of b and N. It is normalized such that $\langle G(N,b) \rangle_o = 1$. Within the multiperipheral model, σ_N has a Poisson-like distribution. For large N, this distribution peaks at around $N \approx \bar{N}$, where $\bar{N}$ is the average particle multiplicity, which for large E is given by: $\bar{N} \sim g^2 \ln E$.[9] From Eq. (3) one gets the approximate relation,

$$H(s,b) \approx FE^C \, G(\bar{N},b) \quad . \tag{6}$$

We propose to parameterize $G(\bar{N},b)$ as follows,

$$G(\bar{N},b) = \langle e^{-b_N \sqrt{x^2+\lambda^2}} \rangle_b = \frac{b_N (1 + \lambda \sqrt{b^2+b_N^2})}{(b^2 + b_N^2)^{3/2}} \exp -\lambda [\sqrt{b^2+b_N^2} - b_N] \quad , \tag{7}$$

with

$$b_N = d_1 (\bar{N} - 2) + d_o \quad . \tag{8}$$

To motivate the proposed form of Eq. (7), let us look at the b dependence of the right hand side. In the small b region (i.e. $b \ll b_N$), the exponent can be approximated by the form

$$G(\bar{N},b) \propto \exp[- \frac{b^2}{2(b_N/\lambda)}] \quad . \tag{9}$$

This expression can be linked to the usual random walk picture.[6,10,11] In particular, each emission along the chain for small b appears to contribute to a step in the two-dimensional b space with step-size $(d_1/\lambda)^{\frac{1}{2}}$. All the steps add in a random walk fashion to give rise to a final radius-squared $(\bar{N} - 2)d_1/\lambda$. The parameter d_o in Eq. (8) accounts for contribution of the two external verteces. In the large b region (i.e. $b >> b_N$), the parameterization of Eq. (7) has the property that for fixed s as b increases, the quantity $G(\bar{N},b)$ and in turn the 2-2 elastic partial wave amplitude, fall off like

$$\sim \frac{1}{\sqrt{\ell}} \exp(-\text{const. } \ell) \quad ,$$

where ℓ is the total angular momentum. This has a maximum rate of falloff allowed by a finite range interaction.[12]

Back the the unitarity relation, Eq. (2). Making the approximation that T_{22} is purely imaginary and solving for the quadratic equation we get

$$\text{Im}T_{22} = 1 - \frac{1}{\sqrt{1+H}} \quad . \tag{10}$$

To ensure the amplitude T_{22} to be even under crossing, we make the usual replacement, E by $Ee^{-i\frac{\pi}{2}}$ and write

$$T \equiv T_{22} = i(1 - \frac{1}{\sqrt{1-2iT_o}}) \quad , \tag{11}$$

where T_o is the "Born term" amplitude (note $T_o = \lim_{F\to C} T_{22}$), given by

$$T_o = \frac{iF}{2}\,(Ee^{-\frac{i\pi}{2}})^C\, G(\bar{N},b) \quad . \tag{12}$$

For the complexified version, we choose the parameterization:

$$b_N = B_o[g^2(\ell nE - \frac{i\pi}{2}) + d] \approx B_o[(1 + c)(\ell nE - \frac{i\pi}{2}) + d] \quad , \tag{13}$$

where B_o and d are new parameters. Equations (7), (11), (12) and (13) completely specify the diffractive amplitude. For future convenience, the explicit algebraic form of T is given in the Appendix.

For comparison with the low energy data, we further add a Regge pole contribution to T and write the full elastic amplitude as,

$$A = T + R \quad . \tag{14}$$

The relevant Regge poles for near forward pp scattering are the ω-ρ and the A_2-f^o trajectories. Their contribution is parameterized as[13]

$$R = [-\beta_+(e^{-i\pi\alpha(t)} + 1) + \beta_-(e^{-i\pi\alpha(t)} - 1)]\; E^{\alpha(t)-1}\; e^{at} \quad , \tag{15}$$

with the "±" subscripts designating the even and odd signatures

and $\alpha(t) = \frac{1}{2} + t$. In the limit of exchange degeneracy, $\beta_+ = \beta_-$. Due to the oversimplified parameterization for the nondiffractive term, we will not impose this relation for R.

3. Comparison with the data.

We make use of the normalization convention,

$$\sigma_T \approx 4.41 \ \mathrm{Im}A \quad \text{(in mb)} \ , \qquad (16)$$

$$\text{and } \frac{d\sigma}{dt} = |A|^2 \quad \text{(in mb/GeV}^2\text{)} \ .$$

Present model was used to carry out a simultaneous fit to pp data: σ_T and Re/Im at t = 0, the slope parameter of differential cross section at t = 0 and t = -0.35 and some sample differential cross sections at 12.8, 19.2 and 1500 GeV/c. To further constraint Regge pole residues, $\bar{p}p$ total cross section data are also included in the fit. For the pp case, the factor "β_-" in Eq. (15) is replaced by "$-\beta_-$". No least-square fit program was used, although sample calculations were made with parameters varied to obtain their optimum values. We present a typical solution here. The parameters are:

<u>diffractive part</u>	<u>Regge pole part</u>
F = 50.0	
$\lambda = 0.44$ mb$^{-\frac{1}{4}}$ GeV$^{\frac{1}{2}}$	$\beta_+ = 10.55$ mb$^{\frac{1}{2}}$/GeV
$B_0 = 0.123$ mb$^{\frac{1}{4}}$/GeV$^{\frac{1}{2}}$	$\beta_- = 4.8$ mb$^{\frac{1}{2}}$/GeV
c = 0.04	$a = 1.75$ GeV^{-2}
d = 13.0	

The comparison of present solution with pp and $\bar{p}p$ total cross section is shown in Fig. 1. Solid curves are theoretical predictions. One sees that fits are reasonable down to $p_{Lab} \sim 6$ GeV/c. The diffractive term alone is also shown in the figure as the dashed curve.

From Eq. (7), for very large s, the partial wave amplitude has a characteristic cutoff in b at

$$\begin{aligned} b^2 &\sim \{[\ell n(FE^c)]^2 + 2\lambda b_N \ell n(FE^c)\}/\lambda^2 \\ &\sim \{(\ell nE)^2[c^2 + 2\lambda B_o c(1+c)] \\ &\quad + \ell nE[2c\ \ell nF + 2\lambda B_o(1+c)\ell nF + 2\lambda B_o cd]\}/\lambda^2 \\ &\tilde{\sim} \{0.006\ (\ell nE)^2 + 0.81\ (\ell nE)\}/\lambda^2 \end{aligned} \tag{18}$$

ignoring some $\ell n \ell nE$ factors. In the last step our solution was used. The numbers imply, for example, at $E \tilde{\sim} 7\times10^5$ GeV/c the first term is only one tenth of the second term, and at $E \tilde{\sim} 2\times10^{29}$ GeV/c, the first term is half of the second term. So the total cross section rises more or less linearly over a long range of E, although ultimately it goes like $\sim(\ell nE)^2$. According to Fig. 1, the present solution predicts a $\sim$7mb rise between $p_{Lab} \sim 1500$ GeV/c and 8×10^4 GeV/c (a characteristic energy for the Isabelle machine).

The comparison between predicted Re/Im ratio of the forward scattering amplitude and the data is shown in Fig. 2. The fit is good at least for p_{Lab} beyond 10 GeV/c. Notice the diffractive component alone gives a positive contribution. Thus it is the nondiffractive term which is responsible for the substantial negative ratio in the low energy region. For completeness, the prediction for $\bar{p}p$ is also included in the plot.

The situation of energy dependence of slope parameter B as defined in the Appendix is shown in Fig. 3. The theoretical curves are evaluated at t = 0 and at t = -0.35. They are to be compared with those points given in the corresponding regions. There is a crude agreement down to $s = 10\ GeV^2$ or $p_{Lab} \gtrsim 4$ GeV/c. Note the definite difference between the slope parameter at t = 0 and that at t = -0.35. This difference already exists at the Born-term level, where the corresponding slope parameter is given by

$$B_{Born} = \frac{Reb_N}{\sqrt{-t+\lambda^2}} \tag{19}$$

Our solution has $\lambda = 0.44 \gtrsim 3m_\pi$. So B_{Born} varies rapidly near t = 0. Apparently after the absorption and unitarization, this feature of varying slope persists to the extent giving a good description to the data.

The situation for differential cross section is illustrated in Figs. 4a and 4b. The fit at ISR region in the small $|t|$

interval is particularly satisfactory. This for p_{Lab} = 1500 GeV/c is illustrated in Fig. 4a. The well advertized "break" in the differential cross section is well reproduced within the model. Fig. 4b illustrates the differential cross sections at various energies. Fits to 12.8 and 19.2 data as shown are satisfactory up to $|t| \lesssim 0.8$ GeV^2. At 1500 GeV/c, the predicted curve deviates from the data also at around $|t| \lesssim 0.7$ to 0.8. It has a dip at $|t| \lesssim 0.9$ GeV^2, while the data shows a dip much further out in $|t|$. In particular it is at $|t| \lesssim 1.2$ GeV^2.

The predicted differential cross section at Isabelle energy is also shown in Fig. 4b. Three features are particularly worth noting:

(i) the rapid shrinkage phenomena,

(ii) the inward motion of the dip, and

(iii) the rise of the secondary maxima.

Our fits to elastic data and asymptotic predictions are similar to those obtained from the impact picture parameterization reported in refs. 7 and 16, except for the latter no detail fits to the slope parameter, Re/Im and the differential cross section data below, say $s \lesssim 100$ GeV^2, were made. In ref. 7, fits to ISR differential cross section are extended much further out in t. Within the present framework, it appears necessary to look for a different parameterization for $G(\bar{N},b)$, in order to reproduce the observed larger $|t|$ behavior. We have not yet explored this possibility. Anyhow,

at least for $|t| \lesssim 0.8$ GeV^2, where most of the cross section is, we found that, both models give similar description to the elastic data. In other words, the elastic data for $|t| \lesssim 1$ is insensitive in distinguishing the two models. The multiparticle production information is a more rewarding place to investigate the differences of the two models. We shall come to this later on.

4. Discussions.

4.1. The smallness of c. In Sec. 2, the trajectory zero-intercept $\alpha(0) = \frac{1}{2}$, was assumed from the very start. We examine now the implication for the different choices of $\alpha(0)$. Let N_o be the average number of decayed pions per particle which is being emitted along the multiperipheral chain. The data gives[17]

$$\bar{N}_\pi \gtrsim 2.3 \ln E \quad . \tag{20}$$

On the other hand, the multiperipheral model predicts

$$\bar{N} \equiv \frac{\bar{N}_\pi}{N_o} \sim g^2 \ln E \quad . \tag{21}$$

Thus

$$N_o \gtrsim \frac{2.3}{g^2} = \frac{2.3}{2 - 2\alpha(0) + c} \tag{22}$$

With $c = 0.04$,

$$\begin{aligned} &\text{for } \alpha(0) = 1 \ , \quad N_o = 57 \ , \\ &\qquad \alpha(0) = \tfrac{1}{2} \ , \quad N_o = 2.2 \ , \\ &\text{and } \alpha(0) = 0 \ , \quad N_o \simeq 1.1 \ . \end{aligned} \tag{23}$$

If one assumes that N_o is not much more than 2 (or 3), the present solution then definitely favors building up the

diffractive contribution through the exchange of the aforementioned "proper trajectories." The exchange of objects with intercept around unity would necessarily implicate the emission of clusters which subsequently decay into an unreasonably large number of pions.

A short-coming of our proposal is that we have not given an explicit multiperipheral amplitude from which to deduce the b-dependence of the G-function assumed. So we are not able to extract the inclusive distribution from the model. Recently, in the context of an unabsorbed multiperipheral model, an intriguing relation between the average particle transverse momentum $\langle p_\perp^2 \rangle$, the slope parameter of the elastic cross section at t = 0, and the average particle multiplicity was derived.[10,11] In the derivation, some simplified assumptions and asymptotic approximations were made. Apparently a gross discrepancy between the prediction of the unabsorbed multiperipheral model and the data was found. It is unclear, a priori, whether a similar criticism should be applied to the present work.

4.2. Comparison with the eikonal model in the multiparticle production phenomena. We observe that the leading asymptotic term of the "generating function" for a multiperipheral model can be cast in the general form[18]

$$H(x,b) \sim \exp[g_1(x)\ \ell nE + g_2(x)]\cdot F_{\bar{N}}\ (b) \quad , \qquad (24)$$

where x in this subsection represents the dummy variable which keeps track of the number of pions in the final state. Taking into account the initial and final state absorptions between the two nucleons, the absorbed inelastic cross section is given by

$$\sigma_{in} = \sigma_{in}(x)\big|_{x=1} = \langle |S|^2 \ (|S(x,b)|^2 - 1)\rangle_o \qquad (25)$$

To see the role of x for example, by expanding the right hand side in powers of x, one obtains the topological cross section. In particular, σ_N can be read off directly from the coefficient of x^{N-2}.

For eikonal models[3,5]

$$\sigma_{in}(x) = \langle |S|^2 \ (e^{H(x,b)} - 1)\rangle_o \quad . \qquad (26)$$

Thus the average pion multiplicity is given by

$$f_1^{eik} = \frac{1}{\sigma_{in}} \frac{d\sigma_{in}(x)}{dx}\Big|_{x=1} = \langle N_\pi^L \rangle \langle N_L \rangle \quad , \qquad (27)$$

Equation (24) gives with $g^{2\prime} = \frac{dg^2}{dx}$,

$$\langle N_L \rangle = F \cdot E^{g_1^2(1)} \ e^{g_2^2(1)}/\sigma_{in}, \ \langle N_\pi^L \rangle = g_1^{2\prime}(1) \ \ell n E + g_2^{2\prime}(1) \quad , \qquad (28)$$

where $\langle N_L \rangle$ is the average number of "open ladders" produced[2,3,4] while $\langle N_\pi^L \rangle$ is the average number of pions in each open ladder.

The strong coupling conditicn says $g_1^2(1) > 0$. So Eq. (27) now implies that the growth of $\langle N_L \rangle$ will eventually dominate over the growth of $\langle N_\pi^L \rangle$. Furthermore, the overall pion multiplicity grows like $\sim E^{g_1^2 \ell nE/\sigma_{in}}$, or ultimately $\sim E^{g_1^2/\ell nE}$.

For the present model, taking the same parameterization as that given in Eq. (24), we get

$$f_1 = g_1^{2\prime}(1) \ \ell nE + g_2^{2\prime}(1) \quad . \tag{29}$$

Thus the energy dependence of the pion average multiplicity is one place where one can distinguish between the eikonal-type model and the present model. Our preliminary investigation on topological distributions also indicates that the two models give very different predictions there. Detail theoretical investigation on the topological distribution may prove to be useful to further specify ways to distinguish the two models.

We thank Professor E.C.G. Sudarshan for encouraging us to look into the ultra high energy physics in connection with the Isabelle project study. This originally instigated the present investigation.

Footnotes and References

1. Pisa-Stony Brook collaboration, Phys. Letters 44, 119 (1973); Rome-CERN collaboration, Phys. Letters 44, 112 (1973).
2. H. Cheng and T. T. Wu, Quantum Electrodynamics at High Energies, Int. Symp. on electron and photon interactions at high energies, Cornell University, p. 148. See also previous papers quoted therein.
3. S. J. Chang and T. M. Yan, Phys. Rev. Letters 25, 1586 (1970); ibid., Phys. Rev. D4, 537 (1971).
4. J. R. Fulco and R. L. Sugar, Phys. Rev. D4, 1919 (1971); S. Auerbach, R. Aviv, R. Sugar and R. Blankenbecler, Phys. Rev. D6, 2216 (1972).
5. J. Finkelstein and F. Zachariasen, Phys. Letters 34B, 631 (1971).
6. L. Caneschi and A. Schwimmer, Nuclear Phys. B44, 31 (1972).
7. H. Cheng, J. K. Walker and T. T. Wu, Phys. Letters 44B, 97 (1973).
8. H. Harari, Phys. Rev. Letters 20, 1395 (1968); P.G.D. Freund, Phys. Rev. Letters 20, 235 (1968).
9. D. Amati, S. Fubini and A. Stanghellini, Nuovo Cimento 26, 896 (1962); G. F. Chew and A. Pignotti, Phys. Rev. 176, 2112 (1968); C. E. De Tar, Phys. Rev. D3, 128 (1971).
10. R. Hwa, "Slope of the forward peak: an s-channel analysis", University of Oregon preprint, 1973.

11. C. J. Hamer and R. F. Peierls, "Transverse momenta and overlap functions in multiperipheral models", Brookhaven National Laboratory preprint, 1973.

12. P.D.B. Collins and E. J. Squires, Regge pole in particle physics, Berlin-Springer, 1968, p. 82.

13. For a review on the parameterization of Regge pole contribution, see for example: C. B. Chiu, Ann. Rev. of Nucl. Sci. 22, 255 (1972).

14. The pp data.

(1) Total cross section.

6-22 GeV/c: W. Galbraith et al., Phys. Rev. 138B, 913 (1965); 15-60 GeV/c: S. P. Denisov et al., Phys. Letters 36B, 415 (1971); 300-1500 GeV/c: see ref. 1.

(2) Re/Im. (See also Giacomelli's review of (3), p. 286.)

5, 7 GeV/c: A. R. Clyde, Ph.D. Thesis, U. C. Berkeley, 1966; 8 GeV/c: A. E. Taylor et al., Phys. Letters 14, 54 (1965); 10, 19 and 26 GeV/c: G. Bellettini et al., Phys. Letters 14, 164 (1965); 9-70 GeV/c: G. G. Beznogikh et al., Phys. Letters 39B, 411 (1972).

(3) Slope parameter.

Data points are taken from Fig. 14 of Giacomelli's review paper, Proceedings of the 14th Int. Conf. on High Energy Physics, vol. 3, p. 288.

(4) Differential cross section.

12.8 GeV/c: K. J. Foley et al., Phys. Rev. Letters 11, 425 (1963); 19.2 GeV/c: J. V. Allaby et al., Phys. Letters 28, 67 (1968); 1500 GeV/c (ISR 26.7 + 26.7

GeV/c): The $|t| \lesssim 0.4$ data is from G. Barbiellini et al., Phys. Letters 39B, 663 (1972); the $|t| > 0.6$ GeV^2 data is by Aachen-CERN-Harvard-Geneva-Torino collaboration, taken from Fig. 2 of ref. 7.

15. The $\bar{p}p$ total cross section data.
6-8 GeV/c: W. Galbraith et al., Phys. Rev. 138B, 913 (1965);
20-65 GeV/c: J. V. Allaby et al., Phys. Letters 30B, 500 (1969).

16. H. Cheng, J. K. Walker and T. T. Wu, Phys. Letters 44B, 283 (1973).

17. For example, the present negative pion average multiplicity data can be represented by $f_1^- = -1.30 + 0.77\ \ell n p_{Lab}$ (see Chiu and Wang, Univ. of Texas, CPT preprint, CPT 176, 1973). This in turn leads to $f_1^\pi \approx 3f_1^- \sim 2.3\ \ell n p_{Lab}$. Our value 2.3 here could be somewhat underestimated.

18. For a discussion on multiperipheral model including the ispin structure, see for examples: G. F. Chew and A. Pignotti of ref. 9; also L. Caneschi and A. Schwimmer, Phys. Rev. D3, 1588 (1971).

Appendix: Algebraic form of the diffractive amplitude

Starting from Eq. (11),

$$T_{22} = -\frac{1}{\sqrt{r}} \sin\frac{\theta}{2} + i\left(1 - \frac{1}{\sqrt{r}} \cos\frac{\theta}{2}\right) \quad , \tag{A-1}$$

where

$$re^{i\theta} = 1 - 2iT_o = (1 + 2ImT_c) - i2ReT_o \quad .$$

The Born-term amplitude T_o is specified in Eq. (12), which gives

$$2T_o = iF(Ee^{-\frac{i\pi}{2}})^c \frac{b_N(1 + \lambda\sqrt{b^2+b_N^2})}{(b^2 + b_N^2)^{3/2}} \exp\left[-\lambda(\sqrt{b^2+b_N^2} - b_N)\right] \tag{A-2}$$

$$\equiv r_5 e^{i\theta_5} \quad ,$$

where

$$r_5 = \frac{FE^c\, r_1 r_2 r_4}{r_3} \quad , \quad \text{and } \theta_5 = \frac{\pi}{2}(1 - c) + \theta_1 + \theta_2 - \theta_3 + \theta_4 \tag{A-3}$$

with the auxiliary variables defined in the following manner

(i) $r_1 e^{i\theta_1} = b_N$. So

$$r_1 = B_o\{[(1 + c)\ell nE + d]^2 + [\frac{\pi}{2}(1 + c)]^2\}^{\frac{1}{2}}$$

$$\text{and } \theta_1 = tg^{-1}\left[\frac{-\frac{\pi}{2}(1 + c)}{(1 + c)\ell nE + d}\right] \quad . \tag{A-4}$$

(ii) $r_2 e^{i\theta_2} = 1 + \sqrt{b^2+b_N^2}$. So

$$r_2 = \sqrt{dx^2+dy^2} \quad \text{and} \quad \theta_2 = tg^{-1}\frac{dy}{dx} \ , \tag{A-5}$$

with $dx = 1 + \lambda d_1 \cos\phi_1$, and $dy = \lambda d_1 \sin\phi_1$,

where $d_1 = [(b^2 + r_1^2 \cos 2\theta_1)^2 + (r_1^2 \sin 2\theta_1)^2]^{\frac{1}{4}}$,

and $\phi_1 = \frac{1}{2} tg^{-1} \dfrac{r_1^2 \sin 2\theta_1}{b^2 + r_1^2 \cos 2\theta_1}$.

(iii) $r_3 e^{i\theta_3} = (b^2 + b_N^2)^{3/2}$. So

$$r_3 = d_1^3 \text{ and } \theta_3 = 3\phi_1 \ . \tag{A-6}$$

(iv) $r_4 e^{i\theta_4} = \exp[-\lambda(\sqrt{b^2+b_N^2} - b_N)]$. So

$$r_4 = \exp[-\lambda(d_1 \cos\phi_1 - r_1 \cos\phi_1)] \tag{A-7}$$

$$\text{and } \theta_4 = -\lambda(d_1 \sin\phi_1 - r_1 \sin\phi_1) \ .$$

The amplitude at arbitrary t is given by

$$T_{22}(s,t) = \int_0^\infty bdbJ_o(xb)\ T_{22}(s,b), \text{ with } x = \sqrt{-t} \tag{A-8}$$

At $t = 0$, $J_o(xb) = J_o(0) = 1$. The slope parameter is defined by

$$B = \frac{d}{dt}\left(\ell n \frac{d\sigma}{dt}\right) = 2[\mathrm{ReA}\ \frac{d}{dt}\ \mathrm{ReA} + \mathrm{ImA}\ \frac{d}{dt}\ \mathrm{ImA}]/\ \frac{d\sigma}{dt} \ , \tag{A-9}$$

where

$$\frac{dA}{dt} = \int_0^\infty bdbA(s,b)J_1(xb)(\frac{b}{2x}) \quad . \qquad \text{(A-10)}$$

At $t = 0$, $J_1(xb)(\frac{b}{2x}) = \frac{b^2}{4}$. In practice Eqs. (A-8) and (A-10) are calculated through numerical integrations.

Figure Captions

Fig. 1. The pp and $\bar{p}p$ total cross section for incident laboratory energy from 5 to 10^5 GeV/c. Solid curves are model predictions. The dashed curve represents diffractive term alone. For data points, see refs. 14 and 15.

Fig. 2. The ratio of the real part to the imaginary part of the pp and $\bar{p}p$ forward amplitude from 5 to 10^5 GeV/c. Solid curves are model predictions. The dashed curve represents diffractive contribution alone. Data points are for pp only. See ref. 14 for detail references.

Fig. 3. The slope parameter B for pp differential cross section in the energy region s = 5 to 2×10^5 GeV^2. Theoretical curves shown are computed at t = 0 and t = -0.35 GeV^2. Data points as shown are divided into two groups: one with $|t| < 0.1$ and the other with $0.15 < |t| < 0.5$. See ref. 14.

Fig. 4. a. A comparison between the theoretical curve and the pp differential cross section data at 1500 GeV/c. For data points see ref. 14.

b. A comparison between theoretical curves and the differential cross section data at 12.8, 19.2 and 1500 GeV/c. For data points, see ref. 14. Prediction at 8×10^4 GeV/c is shown by the dashed curve.

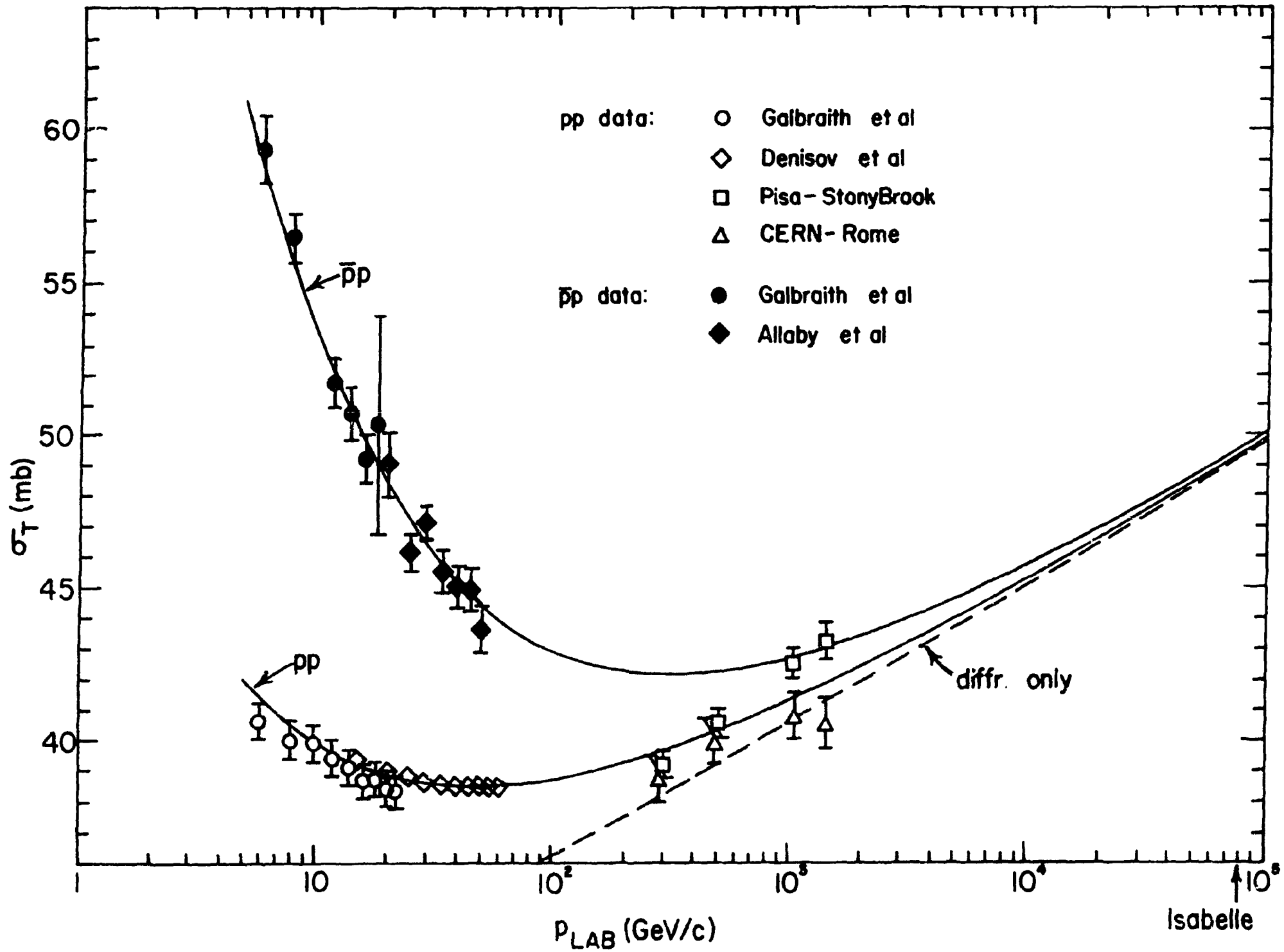
pp data:
Galbraith et al
Denisov et al
Pisa - StonyBrook
CERN - Rome
p̄p data:
Galbraith et al
Allaby et al
p̄p
pp
diffr. only
60
55
50
45
40
σT (mb)
1
10
10²
10³
10⁴
10⁵
Isabelle
P_LAB (GeV/c)

Figure 1

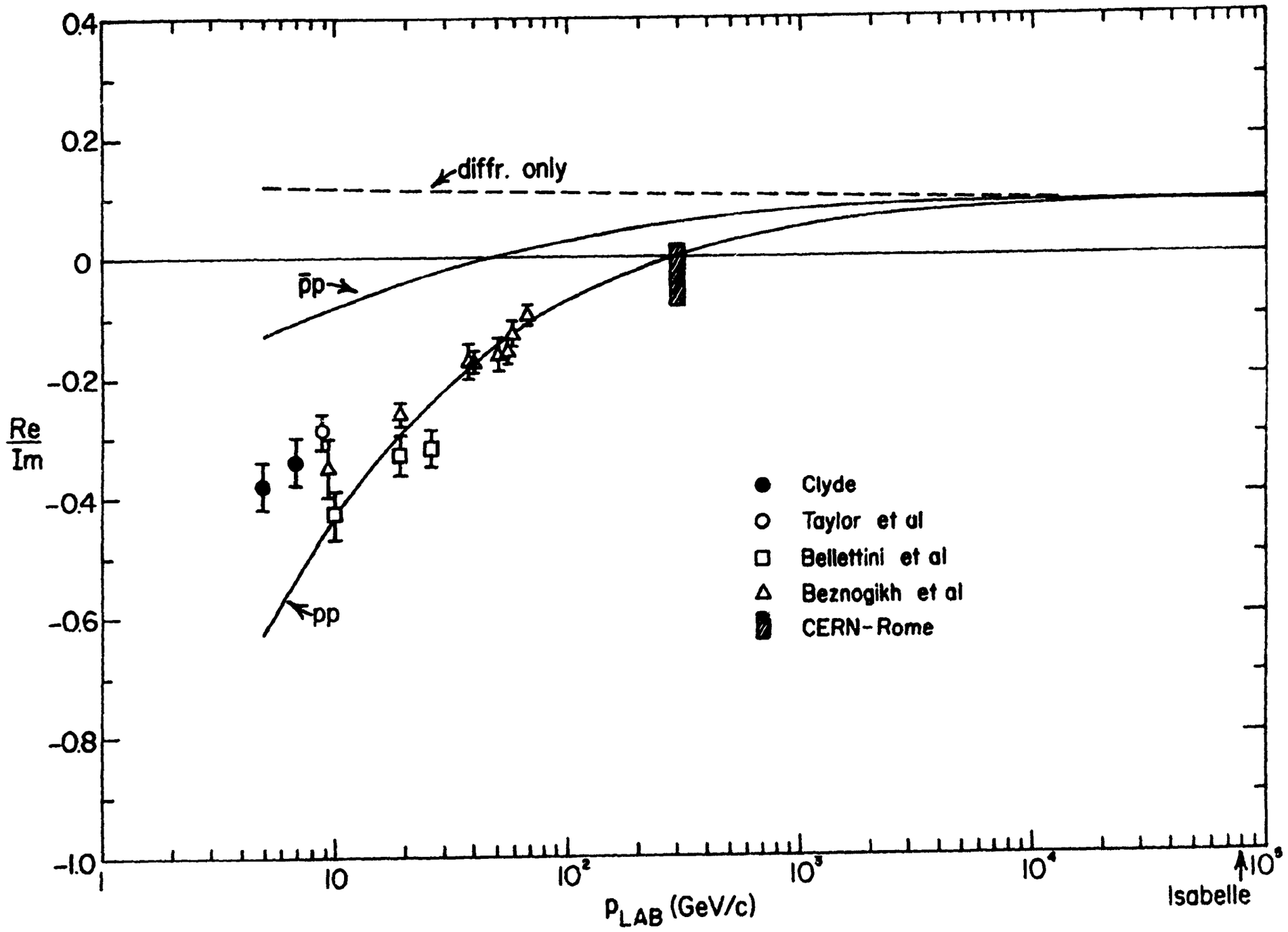
0.4
0.2
0
-0.2
-0.4
-0.6
-0.8
-1.0
Re/Im
diffr. only
p̄p
pp
Clyde
Taylor et al
Bellettini et al
Beznogikh et al
CERN-Rome
1
10
10²
10³
10⁴
10⁵
Isabelle
P_LAB (GeV/c)

Figure 2

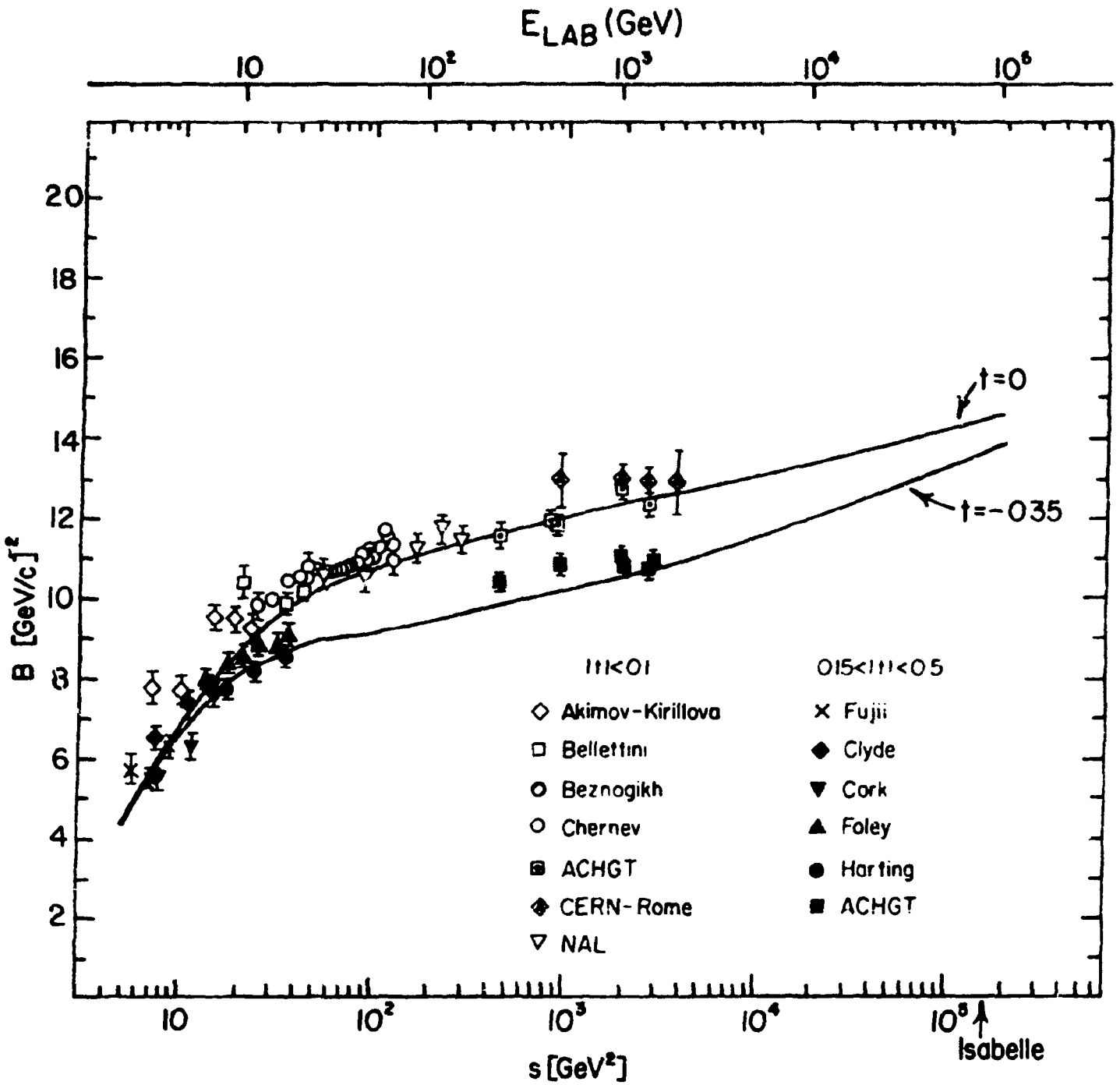
E_LAB (GeV)
10
10²
10³
10⁴
10⁵
20
18
16
14
12
10
8
6
4
2
B [GeV/c]²
t=0
t=-035
|t|<01
015<|t|<05
◇ Akimov-Kirillova
□ Bellettini
○ Beznogikh
○ Chernev
⊞ ACHGT
◈ CERN-Rome
▽ NAL
× Fujii
◆ Clyde
▼ Cork
▲ Foley
● Harting
■ ACHGT
10
10²
10³
10⁴
10⁵
Isabelle
s [GeV²]

Figure 3

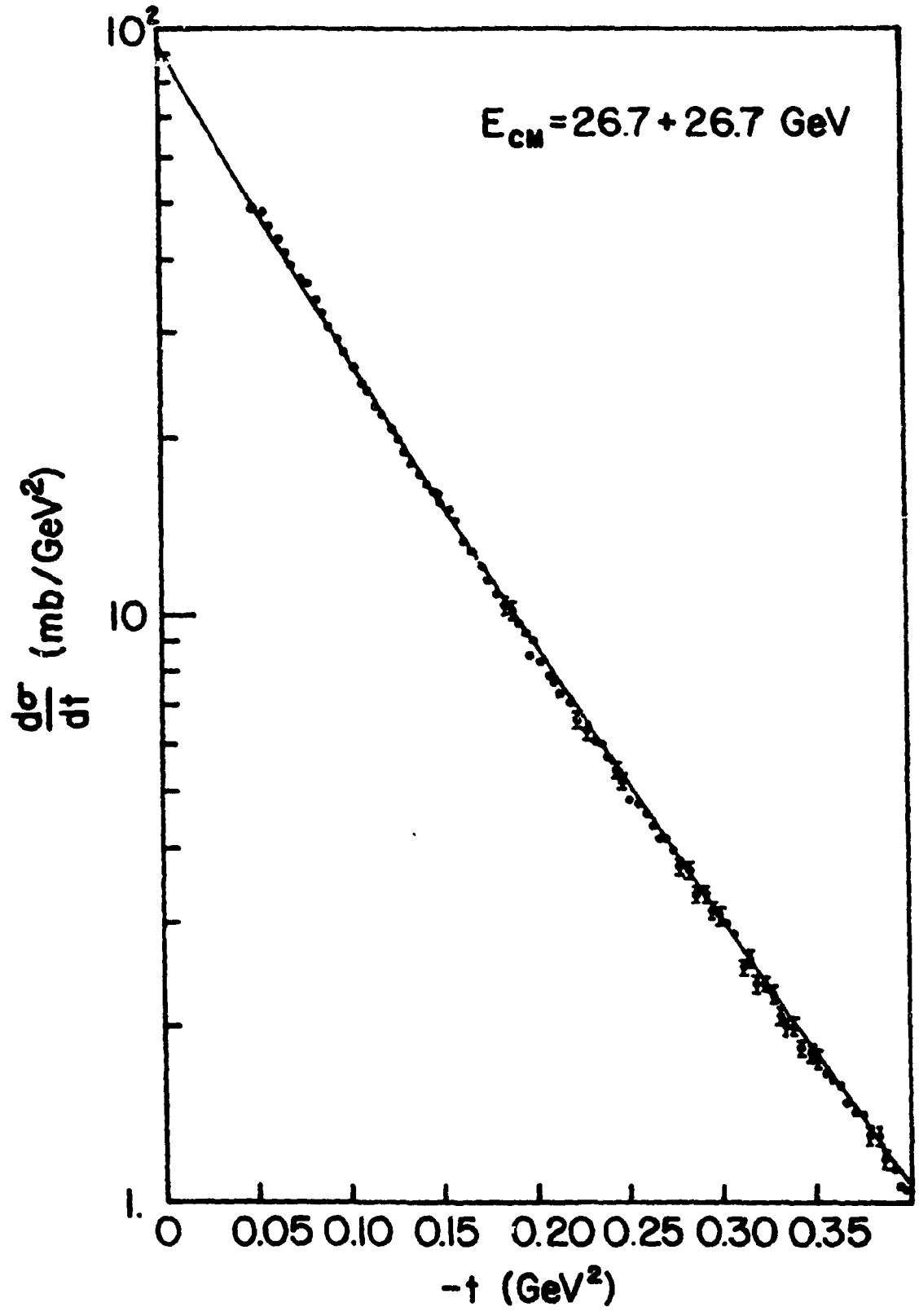
10^2
E_{cM}=26.7+26.7 GeV
$\frac{d\sigma}{dt}$ (mb/GeV^2)
10
1.
0
0.05
0.10
0.15
0.20
0.25
0.30
0.35
-t (GeV^2)

Figure 4a

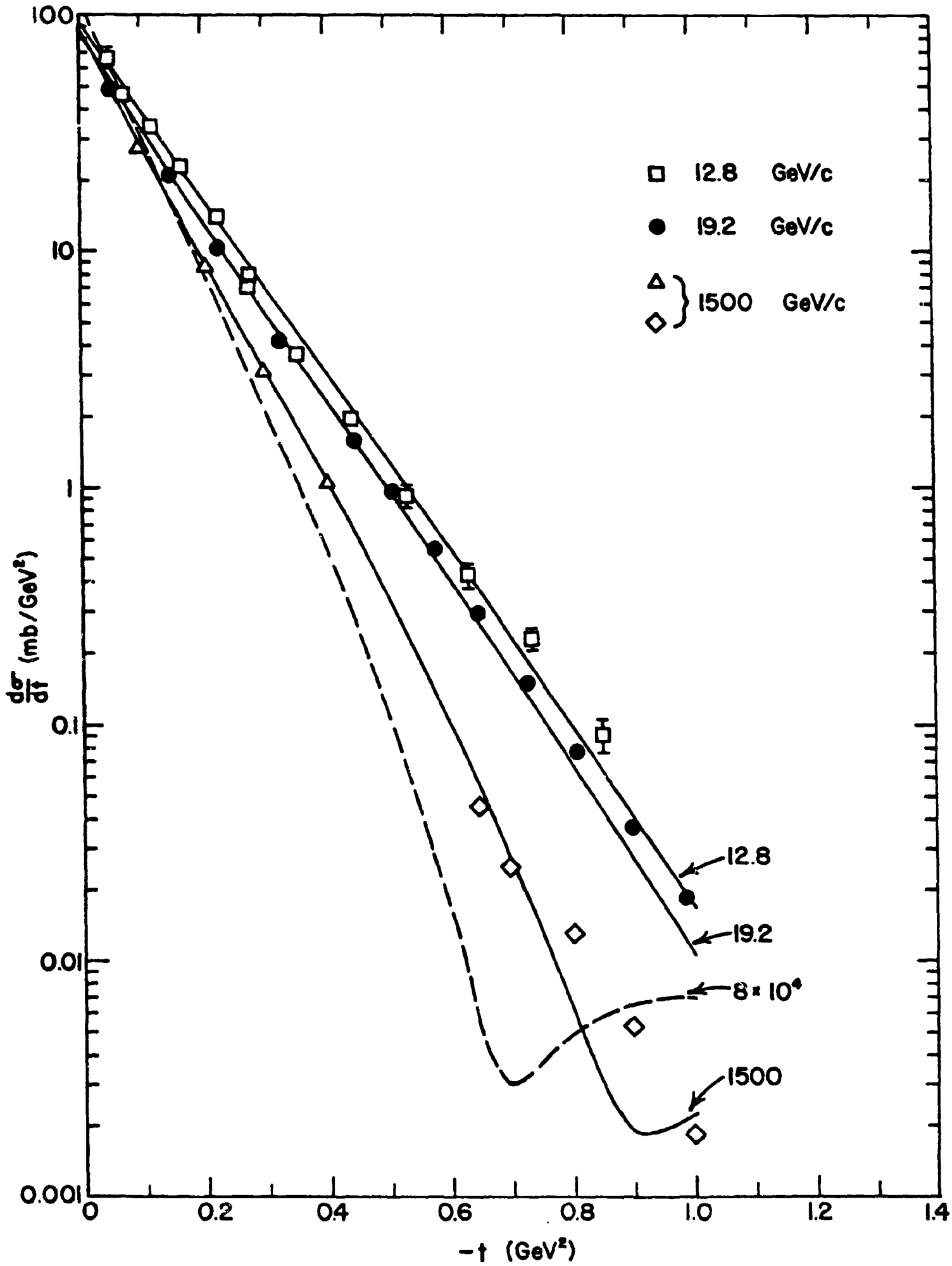
100
10
1
0.1
0.01
0.001
dσ/dt (mb/GeV²)
0
0.2
0.4
0.6
0.8
1.0
1.2
1.4
−t (GeV²)
12.8 GeV/c
19.2 GeV/c
1500 GeV/c
12.8
19.2
8 × 10⁴
1500

Figure 4b